2020-08-03

Numerical Model of a Vertical-Axis Cross-Flow Tidal Turbine

Zhao, R

10.1115/omae2020-18514
Volume 9: Ocean Renewable Energy
American Society of Mechanical Engineers

Proceedings of the ASME 2020 39th International Conference on Ocean, Offshore and Arctic Engineering
OMAE2020
June 28-July 3, 2020, Fort Lauderdale, FL, USA

OMAE2020-18514

NUMERICAL MODEL OF A VERTICAL-AXIS CROSS-FLOW TIDAL TURBINE

Ruiwen Zhao*
Institute for Energy Systems
The University of Edinburgh
Edinburgh EH9 3BF, Scotland, UK
Email: r.zhao@ed.ac.uk

Angus C. W. Creech
Institute for Energy Systems
The University of Edinburgh
Edinburgh EH9 3BF, Scotland, UK
Email: a.creech@ed.ac.uk

Alistair G. L. Borthwick
Institute for Energy Systems
The University of Edinburgh
Edinburgh EH9 3BF, Scotland, UK
Email: alistair.borthwick@ed.ac.uk

Takafumi Nishino
Department of Engineering Science
University of Oxford
Oxford OX1 3PJ, England, UK
Email: takafumi.nishino@eng.ox.ac.uk

Vengatesan Venugopal
Institute for Energy Systems
The University of Edinburgh
Edinburgh EH9 3BF, Scotland, UK
Email: v.venugopal@ed.ac.uk

ABSTRACT

An array of close-packed contra-rotating cross-flow vertical-axis tidal rotors, a concept developed to maximize the fraction of flow passage swept, has potential advantages for hydrokinetic power generation. To predict the commercial feasibility of such rotors in large-scale application, a numerical model of a vertical-axis turbine (VAT) with a torque-controlled system is developed using an actuator line model (ALM). The open-source OpenFOAM computational fluid dynamics (CFD) code is first coupled with this ALM model, and efficiently parallelized to examine the characteristics of turbulent flow behind a vertical axis tidal turbine. The numerical model is validated against previous experimental measurements from a 1:6 scale physical model of a three-bladed reference vertical axis tidal turbine at the University of New Hampshire (UNH-RM2). Satisfactory overall agreement is obtained between numerical predictions and measured data on performance and near-wake characteristics, validating the numerical model. Details of the model setup and discussions on its output/results are included in the paper.

Keywords: vertical-axis turbine, actuator line method, torque control, OpenFOAM, tidal energy.

NOMENCLATURE

c	Blade chord (m)
d_i	Smallest distance between a given point and the i^{th} actuator line (m)
f_{L_i}	Lift component per unit span on the i^{th} blade (N/m)
f_{D_i}	Drag component per unit span on the i^{th} blade (N/m)
F_L	Turbine lift forces per unit span (N/m)
F_D	Turbine drag forces per unit span (N/m)
L	Blade length (m)
N_{bl}	Number of blades
p	Pressure (Pa)
Re	Reynolds number
T	Thrust (N)
u	Local inflow velocity (m/s)
u_0	Freestream velocity (m/s)
u_{bl}	Blade velocity (m/s)

u_{rel}	Flow relative velocity (m/s)
α	Angle of attack (rad)
β	Corrected pitch (rad)
ρ	Fluid density (kg/m^3)
ν	Kinematic viscosity (m^2/s)
η_i	Gaussian regularization
θ	Azimuthal angle (rad)
τ_{fl}	Fluid torque (N m)
τ_{pow}	Generator torque (N m)
τ_{bl}	Blade torque (N m)

INTRODUCTION

Renewable energy will play a key role in achieving the worldwide commitment to reduce greenhouse-gas emissions while providing adequate energy to users [1]. With long histories of exploitation in Europe and along the Atlantic coast of North America, wind and tidal energy are two renewable energy sources whose technologies have undergone rapid development in recent years [1]. Tidal energy is more predictable than wind energy, and has significant potential for future power generation. Although the commercial application of tidal power technology was previously held back by high capital and maintenance costs and technological challenges related to installation, recent improvements in turbine technology have facilitated higher total availability of tidal power at lower economic and environmental costs. It is believed that tidal stream generation is the cheapest and least ecologically damaging of the various forms of tidal power generation [2]. Much ongoing research is being directed towards the development of efficient, reliable tidal stream turbines. Of the different types of tidal stream device that have been invented, cross-flow turbines are particularly attractive because they facilitate much larger flow blockage (or sweepage), and hence power extraction, than other forms of device. Salter [3] compared the performance of cross-flow vertical-axis tidal turbines with axial-flow horizontal-axis tidal turbines in terms of flow impedance, turbulence, blockage ratio, installation, pitch change, and navigation, with the Pentland Firth in mind. Salter and Taylor [4] found that high blockage, vertical-axis, variable-pitch rotors could lead to significantly higher potential power generation for high impedance flows in a duct. Vertical-axis turbines appear to offer a promising near-term technology for tidal energy.

Initial study of vertical-axis turbine (VAT) technology began in the 1970s at Sandia National Laboratories, US, where researchers investigated different vertical-axis turbine configurations, including Savonius (torque generated from drag) and Darrieus (torque generated from lift) turbines [5]. It was found that Darrieus-type turbines have higher cut-in speed than equivalent Savonius turbines and can attain higher coefficients of performance [6][7], even though their support arms introduce additional aerodynamic drag [8]. To solve this problem, Salter and Taylor [4] designed a group of close-packed contra-rotating vertical-axis tidal rotors to maximise the fraction of flow passage swept. Small gaps between the rotors contribute to a high blockage fraction allowing power generation well above the Betz limit for rotors in channels [3]. Following Buntine and Pullin [9], the contra-rotation concept is based on two vortices of opposite-sign cancelling each other out, and thus conditioning the flow though the turbine while lowering the turbulence kinetic energy in the wake. To predict the commercial feasibility such devices at large-scale, a numerical model is required.

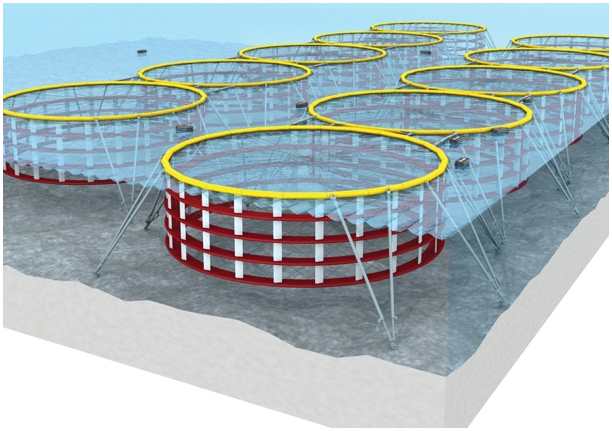

Figure 1: Artist's impression of close-packed vertical-axis contra-rotating rotors [4].

McLaren [10] reported a numerical and experimental study of the unsteady loading on a small-scale, high-solidity, H-type Darrieus turbine, based on 2D, unsteady Reynolds-averaged Navier-Stokes (URANS) simulations by CFD ANSYS-CFX. Nobile et al. [11] simulated 2D unsteady-flow past a Giromill wind turbine using ANSYS CFX. Biadgo et al. [12] used a stream-tube approach to undertake a numerical and analytical assessment of the performance of a vertical-axis wind turbine comprising a straight-bladed fixed-pitch Darrieus turbine with NACA0012 blade profile using ANSYS FLUENT. Bachant et al. [13] developed a validated actuator line model (ALM) of a VAT with both high and a medium solidity, and tested both k–ε RANS and Smagorinsky large eddy simulation (LES) [14][15] turbulence models in the OpenFOAM CFD framework. Compared with other 3D blade-resolved RANS simulations [13][16], Bachant et al.'s model achieved approximately four orders of magnitude reduction in computational expense by implementing corrections in sub-models for the effects of dynamic stall, end conditions, added mass, and flow curvature. Given that such models have focused on idealized VATs, further investigation into optimal practical models is still required.

This paper describes a torque-controlled numerical model of a three-bladed cross-flow vertical-axis tidal turbine, the long-term aim being to model close-packed tidal rotors comprising many blades. The present numerical model is validated against both experimental measurements [13] and numerical simulations [17] of the performance of a 1:6 scale UNH-RM2 tidal turbine. The model is also used to investigate the vorticity distribution in the vicinity of the rotor.

MATHEMATICAL MODEL

Flow past a single vertical-axis turbine (VAT) with an arbitrary number of blades is simulated using an adapted version of the Wind and Tidal Turbine Embedded Simulator (WATTES), which is an efficient, parallelized, two-way coupled turbine model of horizontal-axis turbines, scaling to thousands of computing cores [18][19]. The newly developed model is denoted as WATTES-V. It is a library source code written in Fortran95 and is used to predict the dynamic response to the flow, with lift and drag force components calculated from tabular aerofoil data. A preparatory set-up of the original WATTES model using the OpenFOAM CFD solver has previously been conducted to ensure the codes were correctly coupled [20]. This preliminary work has ensured that WATTES-V model benefits from the advantages of the original model [21].

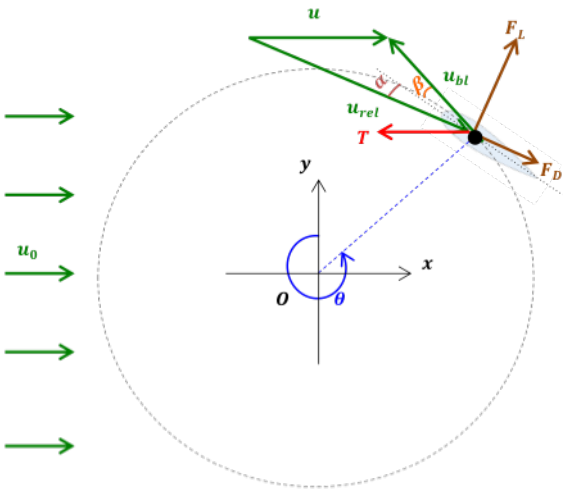

Figure 2: Geometry of and force vectors on a blade of a rotating VAT [21].

The actuator line method (ALM) [22] creates a distribution of body forces along a set of line segments representing the blades of a turbine. Input to WATTES-V comprises the local fluid properties and state, including velocity, flow density, and time, which are passed to the turbine module. For each turbine, nodes are located within the control turbine volume, where the flow velocity relative to the blades u_{rel} and angle of attack α are calculated from the local inflow velocity u, blade velocity u_{bl}, and azimuthal blade angle θ with the corrected blade pitch β. u_0 is the approach flow velocity. Figure 2 shows a schematic diagram illustrating the chord, pitch, and circular trajectory of a single blade, with force component vectors superimposed.

Lift F_L and drag F_D forces are calculated with a two-dimensional Gaussian regularization kernel $\eta_i(d_i)$ from ALM theory in order to determine the torque on fluid τ_{fl}, and the torque that turns the generator to create power τ_{pow} [21],

$$\overrightarrow{F_L} = \sum_{i=1}^{N_{bl}} \eta_i(d_i)\, \overrightarrow{f_{L_i}}, \tag{1}$$

$$\overrightarrow{F_D} = \sum_{i=1}^{N_{bl}} \eta_i(d_i)\, \overrightarrow{f_{D_i}}, \tag{2}$$

where N_{bl} is the number of blades, d_i is the shortest distance between a given point and the i^{th} actuator line, $\overrightarrow{f_{L_i}}$ and $\overrightarrow{f_{D_i}}$ are the pointwise lift and drag per unit span. The calculated force components are then passed back to OpenFOAM as momentum sources in the Navier-Stokes momentum equation for an incompressible Newtonian fluid:

$$\frac{\mathrm{D}\vec{u}}{\mathrm{D}t} = -\frac{1}{\rho}\nabla p + \nu\nabla^2\vec{u} + \frac{1}{\rho}\vec{F}, \tag{3}$$

where $\vec{u}$ is velocity field vector, ρ is fluid density, p is pressure, ν is the kinematic viscosity, t is time, and $\vec{F}$ is the body force vector exerted on the fluid.

The moment of inertia of the rotor is defined with torque to accelerate the blades in WATTES-V. We use moment of inertia to define τ_{bl}, the torque that accelerates the blades. More details of this, and the time integration scheme used, can be found in [19].

TURBINE PARAMETERIZATION

This VAT model with a torque-control system is validated against experimental measurements obtained by Barone et al. [23] from a 1:6 scale physical model of a cross-flow hydrokinetic turbine developed for Sandia National Laboratory, which was tested in the large cross-section tow tank at the Center for Ocean Renewable Energy (CORE) in the University of New Hampshire (UNH), USA [23][24]. The turbine physical model, called UNH-RM2, comprised three rotor blades, each of 1.075 m diameter and 0.8067 m tall. Each rotor blade was constructed with a NACA 0021 profile with the chord tapering from 0.067 m at half-span to 0.04 m at the tip, giving it a solidity, $s = c/R$ (where c is chord length, and R is radius) ranging from 0.12 to 0.07 [13]. The blades were fixed at half-chord and mid-span with 0° preset pitch angle. Further verification is provided by numerical simulations of the 1:6 scale UNH-RM2 vertical-axis turbine model using ALM with RANS by Bachant et al [17]. The turbine is modelled at $Re_D = u_0\, D/\nu \sim 10^6$ (in which D is rotor diameter) for which experimentally measured performance and near-wake characteristics are nearly independent of Reynolds number [13].

Figure 3(a) shows a cross-section sketch of the model turbine and instrumentation installed in the tank. Figure 3(b) is a photograph of the test facility. The experiments were performed in the UNH towing/wave tank, which is 36.6 m long, 3.66 m wide, and 2.44 m deep. The turbine was installed in a support frame, and mounted on the carriage via linear bearings, using a pair of 2.2 kN capacity S-beam load cells to measure total

thrust [13][25]. The model turbine had an approximately 11% blockage ratio based on the frontal area [27]. Table 1 lists the turbine model parameters, derived from [13][26][28].

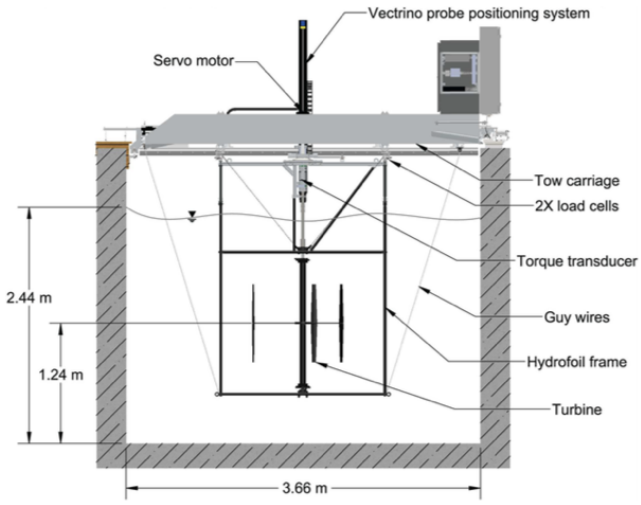

(**a**)

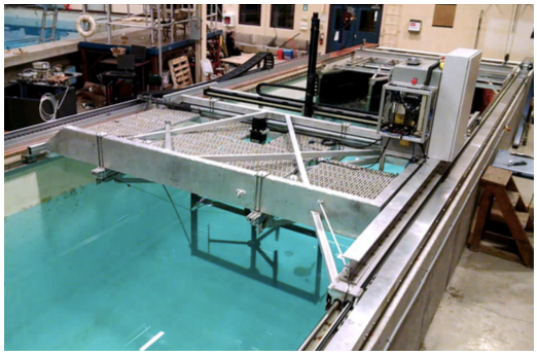

(**b**)

Figure 3: Schematic of experimental setup with the UNH tow tank and turbine test bed with RM2 installed [13]: (a) schematic, and (b) photograph.

The goal of this validation test is to check the ability of the torque-controlled numerical model WATTES-V to predict tidal turbine performance, mean velocity, and turbulence kinetic energy in the near-wake region of the UNH-RM2 turbine at $x = 1D$ downstream. The present numerical model neglects the rotor shaft and support struts, and utilizes an unsteady Reynolds-averaged Navier-Stokes (URANS) formulation with a standard k-ε turbulence closure scheme in OpenFOAM. A similar approach was used by Bachant et al. [17] in their vertical-axis turbine model, whose results are also used for verification here.

Table 1: Model parameters for the three-bladed 1:6 scale UNH-RM2 used to validate the present model.

Property	Symbol	Dimension
Turbine diameter	D	1.075 m
Blade length	L	0.807 m
Aerofoil type	–	NACA 0021
Blade root chord	c_r	0.0667 m
Blade tip chord	c_t	0.04 m
Blade pitch	β_p	0°
Freestream flow speed	u_0	1.2 m/s
Fluid density	ρ	1000 kg/m^3
Local Reynolds number	Re_c	$\sim 10^5$

RESULTS AND DISCUSSION

The present numerical model used a three-dimensional (3D) computational domain that was configured to match the physical tow tank dimensions containing the model-scale tidal turbine. The computational domain comprised a rectangular volume 3.66 m long, 3.66 m wide, and 2.44 m tall, with the turbine located 1.52 m from the inlet, and at a vertical elevation in the centre of the tank depth with its axis oriented vertically [26]. Figure 4 shows a mesh slice in the x-y plane, generated using blockMesh and snappyHexMesh utilities in OpenFOAM. The mesh consists of a hexahedral mesh refined in three dimensions by a factor of 2 in the (n_x, n_y, n_z) directions. Simulations were performed using the pimpleFoam solver, a merged PISO-SIMPLE algorithm.

Initial and boundary conditions were set to approximate those in the physical tow tank test section. The inflow velocity was prescribed to be 1.2 m/s inflow, no-slip lateral and bottom walls fixed to 1.2 m/s, and a frictionless lid applied as a slip condition at the upper boundary to simulate the free surface flow in the tow tank. A zero-pressure gradient was applied at the inlet, and a fixed pressure prescribed at the outlet. The gradients of other flow variables were set to zero at the flow boundaries. The inlet turbulence intensity was $\sim$1.15%, with turbulence kinetic energy k of 2×10^{-4} m^2/s^2, and turbulence dissipation rate ε of 2×10^{-6} m^2/s^3.

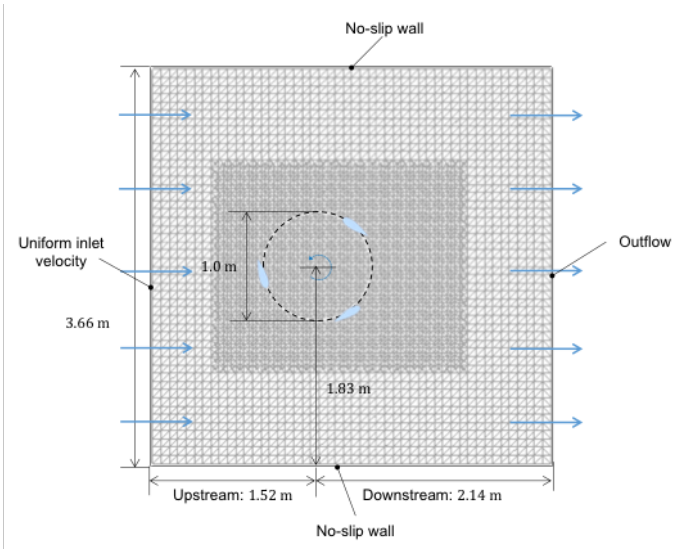

Figure 4: Computational mesh and boundary conditions for a three-bladed vertical-axis tidal turbine, showing plan dimensions of the modelled domain.

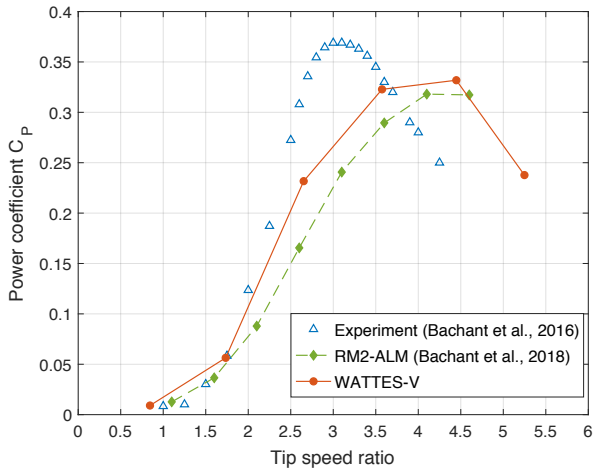

Figure 5: Power coefficient computed for 1:6 scaled UNH-RM2, compared against experimental data [13], a RM2 ALM model [17], and the WATTES-V model with torque-controlled system.

Sensitivity tests were performed regarding spatial and temporal grid resolution, in a similar fashion to the verification strategy employed by [13] at optimal tip speed ratios. The resolution was scaled proportional to the number of cells in the x-direction N_x and was uniform in resolution in all directions. In the RM2 case, $N_x = 48$ and the time step $\Delta t_0 = 0.005$ s (approximately 200 steps per revolution for a tip speed ratio TSR $= 3.1$). The blue blades in Figure 4 are shown for interpretation purposes only, with about 5 cells covering a single blade chord. Both the spatial and temporal resolutions are consistent with the case studies in [13]. The number of steps per revolution was kept constant in order to compute the performance, where the time step is set as $\Delta t = \Delta t_0 \, \mathrm{TSR}_{\mathrm{pk}} / \mathrm{TSR}$ and $\mathrm{TSR}_{\mathrm{pk}}$ is the tip speed ratio corresponding to the experimental peak C_P [17]. Figure 5 shows performance curves relating power coefficient to tip speed ratio obtained using the present dynamic WATTES-V model, measurements from the tow tank experiments [13], and predictions from the RM2 ALM [17]. It can be seen that the present C_P results from WATTES-V are in accordance with predictions by Bachant et al. [17]. The relative two-norm error between the two predicted results is 3.6%, and is within acceptable margins. The slight discrepancy is caused by the lack of struts and support structures in the present WATTES-V mode. The power coefficient C_P is over-predicted at high tip-speed ratio, with a relative two-norm error of 7.69%, and the tip-speed ratio of the peak power coefficient is shifted to the right of the experimental data [13] due to inaccurate modelling of dynamic stall in RM2 ALM [17], as stated by Bachant et al. [17], and the lack of a dynamical stall correction in WATTES-V.

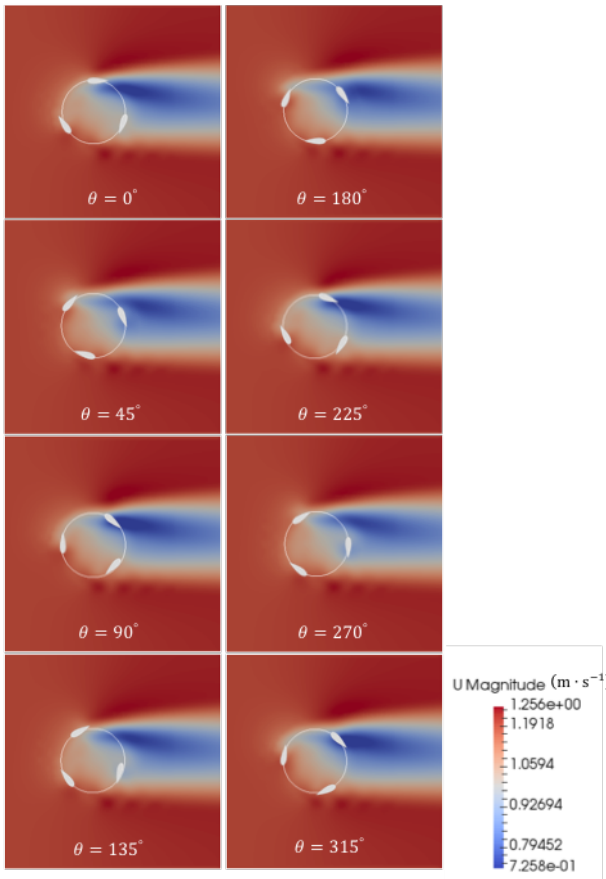

Figure 6(a): Flow patterns at eight different phases during a single revolution for TSR = 3.1 of velocity magnitude (m/s) in the central horizontal x-y plane.

Plan views of the evolving velocity magnitude and instantaneous vorticity z-component in the horizontal x–y plane at eight different phases during one revolution are shown in Figure

6(a) and Figure 6(b) respectively for a 3-bladed tidal turbine operating with torque-control at TSR = 3.1. It can be seen clearly that the blade rotates into the downstream flow, shedding large vortices. Strong tip vortices then interact with the shed vortices, creating a complicated downstream wake field. The value of the z-component of vorticity ranges from 1.23 to 2.69 s^{-1} for TSR from 1.1 to 4.6 considered herein.

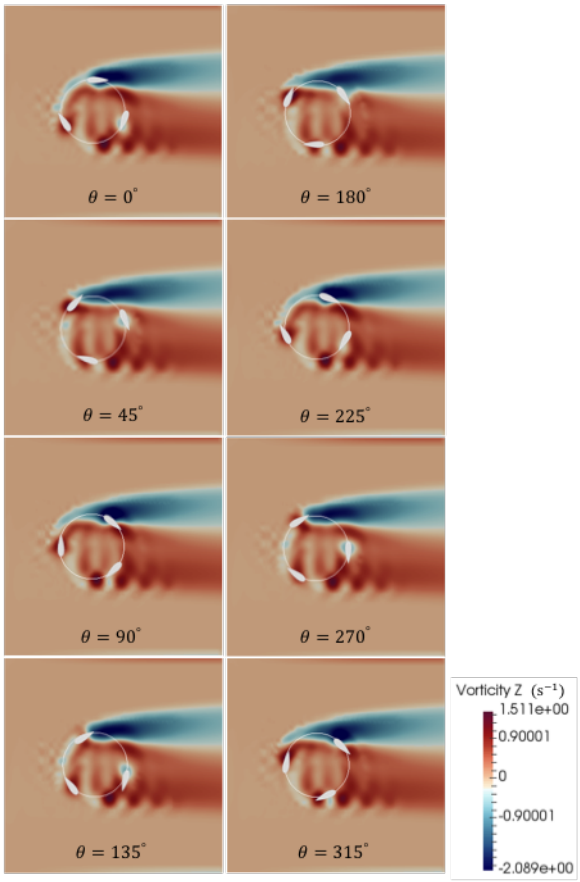

Figure 6(b): Flow patterns at eight different phases during a single revolution for TSR = 3.1 of z-component of vorticity (s^{-1}) in the central horizontal x-y plane.

Plan views of the evolving instantaneous turbulence kinetic energy contours in the horizontal $x-y$ plane at eight different phases during one revolution are shown in Figure 6(c) for a 3-bladed tidal turbine operating with torque-control at TSR = 3.1. The white blades are shown for interpretation. The incoming flow (from left to right, in x-direction) passes through an annulus mapped out by the anti-clockwise rotating three-bladed turbine, with vorticity generated on the surface of the blade and a turbulent wake developing downstream. Vortices detach periodically from the turbine, and move to the downstream low-pressure wake field. This vortex shedding process drives oscillations in the local flow field affecting the forces on the rotor blades and interacting into the downstream wake field.

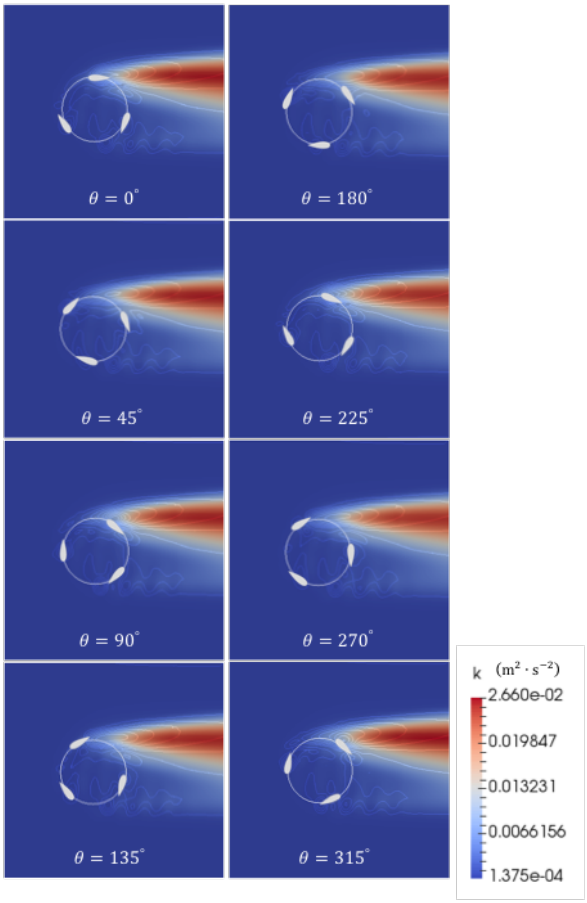

Figure 6(c): Flow patterns at eight different phases during a single revolution for TSR = 3.1 of turbulence kinetic energy (m^2/s^2) in the central horizontal x-y plane with a vorticity contour.

Figure 7 depicts the lateral profiles of stream-wise mean velocity and turbulence kinetic energy in the near-weak region at $x = 1D$, $1.5D$, and $2D$ downstream for TSR = 3.1. The low-momentum area is isolated from the ambient flow in the presence of vortices, where the mean velocity profiles are noticeably asymmetric near the turbine centre. The mean turbulence kinetic energy profiles are in accordance with those of the mean velocity profiles, where the maximum peak of the turbulence kinetic energy is located on the side with positive y, coincident with the lowest velocity deficit. The large vortices shed when the blade motion is in the opposite direction to the flow velocity, play a key role in mixing between the ambient flow and the low-velocity wake flow.

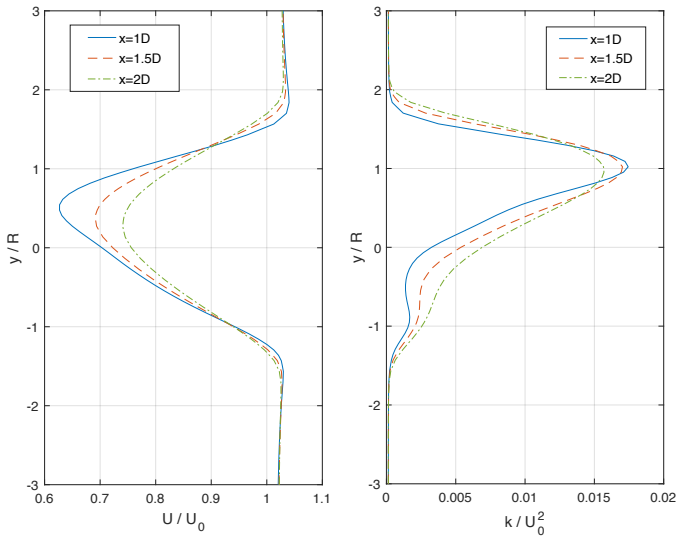

Figure 7: Horizontal profiles at mid-elevation of turbine $z/H = 0$ at TSR $= 3.1$: (**a**) mean stream-wise velocity component; and (**b**) turbulence kinetic energy at $x = 1D$, $x = 1.5D$, and $x = 2D$ respectively.

A parameter study of a pitch control system is presented in the following section, which aims at solving the dynamic stall problem, and providing an even pressure drop across the whole diameter of turbine. The pitch is controlled (and calculated by) using the pressure over the slit width due to the blade lift component and the pressure due to the downstream fluid force [4].

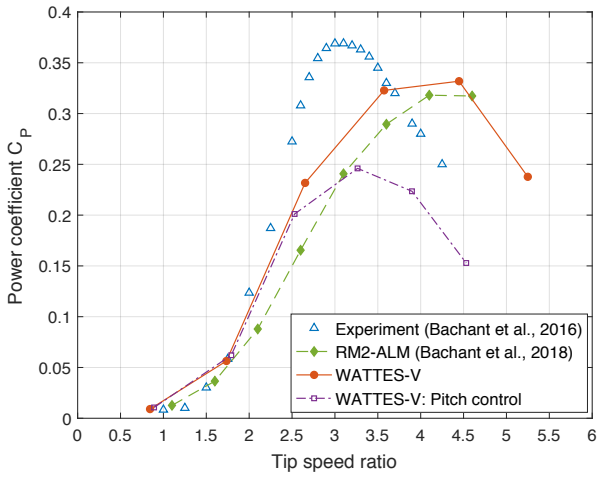

Figure 8: Power coefficient computed for 1:6 scaled UNH-RM2, compared against experimental data [13], a RM2 ALM model [17], the torque-controlled WATTES-V model without pitch control, and the WATTES-V model with pitch control enabled.

Figure 8 shows power coefficient performance curves against tip speed ratios, obtained from tow tank measurements [13][26], predictions from the RM2 ALM numerical model [17], and predictions from the dynamic WATTES-V model with and without pitch control. It can be seen that the pitch control WATTES-V model predicts the tip speed ratio at which the peak power coefficient occurs is rather closer to the experimental data [13][26] than the other predictions from the RM2 ALM model [17] and the WATTES-V model without pitch control. Overall agreement in terms of general trends is obtained between the numerical predictions of a pitch-controlled model and measured data concerning turbine performance. However, the peak in the performance profile predicted by the WATTES-V model with pitch control is much lower than measured experimentally; this underestimate is caused by the limited pitch-control system possible in a turbine with a small number of blades. The amplitude of the predicted profile of the pitch-controlled model is evidently lower than that of the other predicted results when TSR has a higher value. This shows that the pitch controlled by a more uniform distribution of pressure over the whole turbine diameter does not contribute to the power output, and could even have an adverse impact on the performance of a three-bladed vertical-axis turbine.

The pitch angle is also a potential parameter by which to enhance the performance of a vertical-axis turbine [29]. The fact that the pitch angle keeps shifting under the instantaneous loading and moment experienced during the revolution of the rotor blade suggests that dynamic pitching might be a promising approach for future studies of performance optimization [29]. With this in mind, a parameter study of a pitch control system, aimed at enhancing the performance of VATs with a small number of blades, is recommended to be explored in future work.

CONCLUSIONS

This paper has presented a validation of the WATTES-V model of a cross-flow tidal turbine with a torque-controlled system by comparison against experimental results [13] and numerical predictions from an alternative RM2 ALM model [17]. The WATTES-V model predictions displayed satisfactory agreement with both the experimental data and the RM2 ALM model, except for a small deviation in the value of tip-speed ratio at which the maximum power coefficient C_P occurs owing to dynamic stall as the rotor blades revolve.

A parameter study of a pitch control system, providing an even pressure drop across the whole diameter of turbine, has also been explored in this paper. It solves the problem of the tip-speed-ratio deviation where the peak power coefficient C_P occurs. The underestimate of the maximum C_P is caused by the limited pitch-control system possible in a turbine with a small number of blades. A further parameter study of a pitch control system, aimed at enhancing the turbine performance, will be explored in future work.

ACKNOWLEDGEMENTS

The first-named author is supported by funding awarded by the China Scholarship Council and the University of Edinburgh. The authors thank Prof. Stephen Salter for insightful suggestions that have informed the present research.

REFERENCES

[1] Mathew, S., "Wind energy: Fundamentals, resource analysis and economics.", *Wind Energy: Fundamentals, Resource Analysis and Economics*, 2007.

[2] Tidal Streams, "Tidal power", *website: http://www.esru.strath.ac.uk*, 2010.

[3] Salter, Stephen H., "Are Nearly all Tidal Stream Turbine Designs Wrong?", *4th International Conference on Ocean Energy*, 2012.

[4] Salter, S. H. and Taylor, J. R. M., "Vertical-axis tidal-current generators and the Pentland Firth.", *Proceedings of the Institution of Mechanical Engineers, Part A: Journal of Power and Energy*, 2007.

[5] Sutherland, H. J., Berg, D. E., Ashwill, T. D., "A retrospective of VAWT technology.", *Technical Report SAND2012-0304, Sandia National Laboratories, Albuquerque, New Mexico*, 2012.

[6] Sahim, K., Santoso, D., Puspitasari, D., "Investigations on the Effect of Radius Rotor in Combined Darrieus-Savonius Wind Turbine.", *International Journal of Rotating Machinery*, 2018.

[7] Subramanian, A., Yogesh, S. A., Sivanandan, H., Giri, A., Vasudevan, M., Mugundhan, V., Velamati, R. K., "Effect of airfoil and solidity on performance of small scale vertical axis wind turbine using three dimensional CFD model.", *Energy, 133, 179–190*, 2017.

[8] Dyachuk, E., "Aerodynamics of Vertical Axis Wind Turbines - Development of Simulation Tools and Experiments", 2015.

[9] Buntine, J. D. and Pullin, D. I., "Merger and cancellation of strained vortices.", *J. Fluid Mech, 205, 263- 295*, 1989.

[10] McLaren, K.W., "Unsteady loading of high solidity vertical axis wind turbines.", *PhD Thesis*, 2011.

[11] Nobile, R., Vahdati, M., Barlow, J. F., "Unsteady flow simulation of a vertical axis wind turbine: a two-dimensional study.", *TSBE Engineering Doctorate Conference, 1–10*, 2013.

[12] Biadgo, A. M. et al., "Numerical and analytical investigation of vertical axis wind turbine.", *FME Trans. 41(1), 49–58*, 2013.

[13] Bachant, P. and Wosnik, M., "Modeling the near-wake of a vertical-axis cross-flow turbine with 2-D and 3-D RANS.", *Journal of Renewable and Sustainable Energy, 8(5)*, 2016.

[14] Deardorff, J., "A numerical study of three-dimensional turbulent channel flow at large Reynolds numbers.", J*ournal of Fluid Mechanics., 41 (2): 45*, 1970.

[15] Smagorinsky, J., "General Circulation Experiments with the Primitive Equation.", *Monthly Weather Review., 91 (3): 99*, 1963.

[16] Krogstad, P. A. and Eriksen, P. E., "Blind test calculations of the performance and wake development for a model wind turbine.", *Renewable Energy, 50, 325– 333*, 2013.

[17] Bachant, P., Goude, A., Wosnik, M., Moran, K. P., Martner, B. E., Post, M. J., Nygaard, N. G., "Actuator line modeling of vertical-axis turbines.", *Bull. Am. Meteorol. Soc*, 2018.

[18] Creech, A. C. W., Borthwick, A. G. L., Ingram, D., "Effects of support structures in an LES actuator line model of a tidal turbine with contra-rotating rotors.", *Energies, 10, 726*, 2017.

[19] Creech, A. C. W., Früh, W. G., Maguire, A. E., "Simulations of an offshore wind farm using large eddy simulation and a torque-controlled actuator disc model.", *Surv. Geophys., 36, 427-481*, 2015.

[20] Zhao, R., Creech, A. C. W., Borthwick, A. G. L., Nishino, T, "Coupling of WATTES and OpenFOAM codes for wake modelling behind close-packed contra-rotating vertical-axis tidal rotors.", *Proceedings of the 6th Oxford Tidal Energy Workshop*, 2018.

[21] Zhao, R.; Creech, A.C.W.; Borthwick, A.G.L.; Venugopal, V.; Nishino, T. Aerodynamic Analysis of a Two-Bladed Vertical-Axis Wind Turbine Using a Coupled Unsteady RANS and Actuator Line Model. Energies 2020, 13, 776.

[22] Troldborg, N., "Actuator line modeling of wind turbine wakes.", *Mechanical Engineering*, 2008.

[23] Barone, M., Griffith, T., Berg, J., Reference Model 2 : " Rev 0 ", *Rotor Design, 8, 33–41*, 2011.

[24] Bachant, P. and Wosnik, M., "Reynolds Number Dependence of Cross-Flow Turbine Performance and Near-Wake Characteristics.", *Proc. of the 2nd Marine Energy Technology Symposium, 1–9*, 2014.

[25] Sentran, "ZB S Beam Load Cell Datasheet.", 2014.

[26] Bachant, P., Wosnik, M., Gunawan, B., Neary, V. S., "Experimental study of a reference model vertical-axis cross-flow turbine.", *PLoS ONE*, 2016.

[27] Bachant, P. and Wosnik, M., "Performance and near-wake measurements for a vertical axis turbine at moderate Reynolds number.", *American Society of Mechanical Engineers, Fluids Engineering Division FEDSM, 1 B, 1–9*, 2013.

[28] Wosnik, M., Bachant, P., Gunawan, B., Wilson, A., Neary, V. S., "Performance Measurements for a 1 : 6 Scale Model of the Doe Reference Model 2 (RM2) Cross-Flow Hydrokinetic Turbine.", *Proceedings of the 3rd Marine Energy Technology Symposium, 2, 2–5*, 2015.

[29] Rezaeiha, A., Kalkman, I., Blocken, B., "Effect of pitch angle on power performance and aerodynamics of a vertical axis wind turbine.", *Applied Energy, 197, 132–150*, 2017.